

Supplementary Material

Design of donor- π -acceptor type cyclo[18]carbon derivatives for infrared nonlinear optical materials: A theoretical perspective

Jingbo Xu^{a,#}, Jiaojiao Wang^{a,#}, Xiaohui Chen^a, Wenwen Zhao^a, Xiufen Yan^a, Zeyu Liu^{a,*}, Tian Lu^{b,*}, Aihua Yuan^{a,*}

^a*School of Environmental and Chemical Engineering, Jiangsu University of Science and Technology, Zhenjiang 212100, People's Republic of China*

^b*Beijing Kein Research Center for Natural Sciences, Beijing 100024, People's Republic of China*

[#] These authors contributed equally to this work.

*Corresponding author. E-mail: liuzy@just.edu.cn (Zeyu Liu), sobereva@sina.com (Tian Lu), aihua.yuan@just.edu.cn (Aihua Yuan)

Contents:

Figure S1. Conformational superposition of the structures of the studied C ₁₈ derivatives optimized at the ωB97XD/def2-TZVP (orange) and M06-2X/def2-TZVP (blue) levels.....	S4
Table S1. Optimized Cartesian coordinates (in Å) of H-C ₁₈ -H.....	S5
Table S2. Optimized Cartesian coordinates (in Å) of H-C ₁₈ -NO ₂	S6
Table S3. Optimized Cartesian coordinates (in Å) of NH ₂ -C ₁₈ -H.....	S7
Table S4. Optimized Cartesian coordinates (in Å) of NH ₂ -C ₁₈ -NO ₂	S8
Figure S2. Bond-length colored molecular structure of the studied C ₁₈ derivatives...S9	
Figure S3. Simulated infrared (IR) spectrum of the studied C ₁₈ derivatives.....S10	
Table S5. Contributions of the main transition orbitals (MTOs) of crucial excited state involved in maximum wavelength absorption.....	S11
Figure S4. Simulated charge-transfer spectrum (CTS) of the studied C ₁₈ derivatives.....S12	
Figure S5. Isosurface maps of electron density difference (EDD) (isovalue = 0.001) of the studied C ₁₈ derivatives.....	S13
Table S6. Transition energy (ΔE , in eV), oscillator strength (f_0), magnitude of the vector difference between the dipole moment of the ground state and those of the excited state ($ \Delta\mu $, in D), and calculated first hyperpolarizability ($\beta_0^*(-2\omega;\omega,\omega)$, in a.u.) derived from the two-level model for the lowest five excited states of the studied C ₁₈ derivatives.....	S14
Table S7. Total amounts of the first hyperpolarizability ($\beta_0(-2\omega;\omega,\omega)$, in a.u.), projection of the first hyperpolarizability onto the dipole vector ($\beta_{\text{vec}}(-2\omega;\omega,\omega)$, in a.u.), and Cartesian component of the first hyperpolarizability ($\beta_x(-2\omega;\omega,\omega)$, $\beta_y(-2\omega;\omega,\omega)$, and $\beta_z(-2\omega;\omega,\omega)$, in a.u.) in zero-frequency limit ($\lambda = \infty$ nm) and under frequency-dependent fields ($\lambda = 1907$ and 1460 nm) of the studied C ₁₈ derivatives in the gas phase (outside parenthesis) and in cyclohexane solution (inside parenthesis) calculated by analytic derivatives of the system energy (CPKS) method.....	S15

Table S8. Tensorial component of the first hyperpolarizability (in a.u.) in the principal axis of the studied C₁₈ derivatives in zero-frequency limit ($\lambda = \infty$ nm) and under frequency-dependent fields ($\lambda = 1907$ and 1460 nm) of the studied C₁₈ derivatives calculated by both analytic derivatives of the system energy (CPKS, outside parenthesis) and finite field (FF, inside parenthesis)
methods.....S16

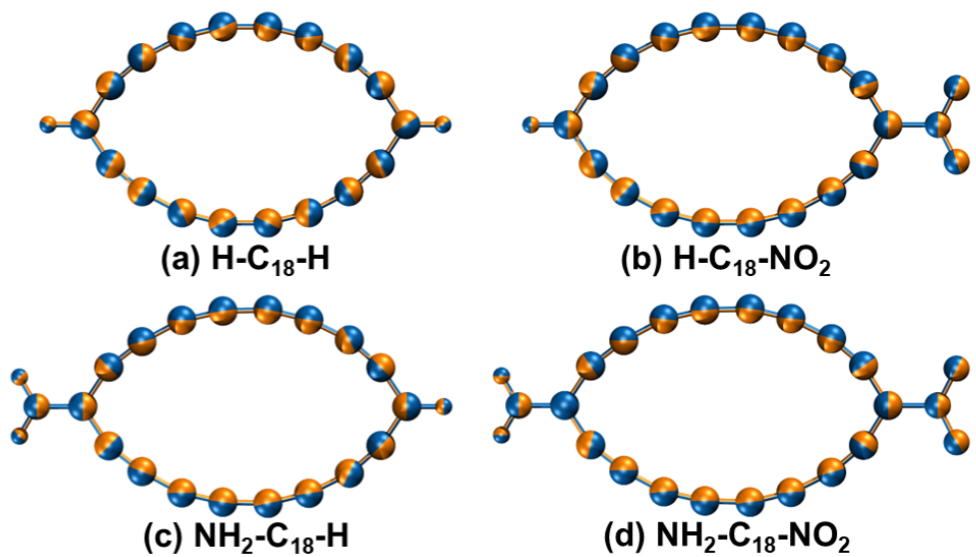


Figure S1. Conformational superposition of the structures of the studied C₁₈ derivatives optimized at the ωB97XD/def2-TZVP (orange) and M06-2X/def2-TZVP (blue) levels.

Table S1. Optimized Cartesian coordinates (in Å) of H-C₁₈-H

atom	x	y	z
C	-0.01939934	2.87539010	0.00015892
C	-1.32922636	2.87518157	0.00041431
C	-2.53569213	2.58384646	0.00042537
C	-3.69818932	1.97586994	0.00034287
C	-4.63124546	1.16215499	0.00017011
C	-5.37608535	0.02662622	-0.00006365
C	-4.62624643	-1.12738898	-0.00010283
C	-3.70554292	-1.93939148	-0.00005871
C	-2.53123623	-2.55837665	-0.00003029
C	-1.33618955	-2.84926088	-0.00000378
C	-0.01051645	-2.84905449	0.00001172
C	1.18443280	-2.55776990	0.00003657
C	2.35852489	-1.93840890	0.00000343
C	3.27894176	-1.12608276	-0.00006831
C	4.02840180	0.02816670	-0.00022287

C	3.28318904	1.16344476	-0.00029242
C	2.34985736	1.97684760	-0.00018158
C	1.18716268	2.58444926	-0.00001903
H	-6.45880962	0.02593260	-0.00017759
H	5.11112645	0.02782392	-0.00034226

Table S2. Optimized Cartesian coordinates (in Å) of H-C₁₈-NO₂

atom	x	y	z
C	-0.43461463	2.85495547	0.00000000
C	-1.75264498	2.85774100	0.00000000
C	-2.95267273	2.56769852	0.00000000
C	-4.12271244	1.95737111	0.00000000
C	-5.04892384	1.14472230	0.00000000
C	-5.79467238	-0.00002024	0.00000000
C	-5.04903447	-1.14483520	0.00000000
C	-4.12290547	-1.95757828	0.00000000
C	-2.95282820	-2.56783462	0.00000000
C	-1.75270629	-2.85748857	0.00000000
C	-0.43467540	-2.85473505	0.00000000
C	0.76678934	-2.57206579	0.00000000
C	1.93464568	-1.95692323	0.00000000
C	2.87832779	-1.16724331	0.00000000
C	3.58496425	-0.00001812	0.00000000
C	2.87828364	1.16718001	0.00000000
C	1.93456787	1.95681931	0.00000000
C	0.76682306	2.57217265	0.00000000
N	5.05112208	0.00000971	0.00000000
O	5.59759963	-1.07958019	0.00000000
O	5.59755867	1.07962035	0.00000000
H	-6.87774803	0.00003218	0.00000000

Table S3. Optimized Cartesian coordinates (in Å) of NH₂-C₁₈-H

atom	x	y	z
C	1.09120281	2.82900416	0.00000000
C	-0.22937222	2.79303525	0.00000000
C	-1.43284668	2.52486927	0.00000000
C	-2.60181801	1.90214127	0.00000000
C	-3.57507737	1.15277480	0.00000000
C	-4.33736453	0.00000000	0.00000000
C	-3.57507737	-1.15277480	0.00000000
C	-2.60181801	-1.90214127	0.00000000
C	-1.43284668	-2.52486927	0.00000000
C	-0.22937222	-2.79303525	0.00000000
C	1.09120281	-2.82900416	0.00000000
C	2.29042829	-2.53858540	0.00000000
C	3.47644300	-1.95500812	0.00000000
C	4.40056747	-1.13983632	0.00000000
C	5.15849772	0.00000000	0.00000000
C	4.40056747	1.13983632	0.00000000
C	3.47644300	1.95500812	0.00000000
C	2.29042829	2.53858540	0.00000000
N	-5.68788870	0.00000000	0.00000000
H	-6.19394091	-0.86483452	0.00000000
H	-6.19394091	0.86483452	0.00000000
H	6.24002319	0.00000000	0.00000000

Table S4. Optimized Cartesian coordinates (in Å) of NH₂-C₁₈-NO₂

atom	x	y	z
C	-0.00945103	2.82317236	0.00000000
C	-1.33366756	2.78971365	0.00000000
C	-2.53462939	2.52406567	0.00000000
C	-3.70685283	1.90083937	0.00000000
C	-4.68063145	1.15622303	0.00000000
C	-5.44311417	0.00000000	0.00000000
C	-4.68063145	-1.15622303	0.00000000
C	-3.70685283	-1.90083937	0.00000000
C	-2.53462939	-2.52406567	0.00000000
C	-1.33366756	-2.78971365	0.00000000
C	-0.00945103	-2.82317236	0.00000000
C	1.18802328	-2.53974044	0.00000000
C	2.37708633	-1.95393431	0.00000000
C	3.31682040	-1.16390563	0.00000000
C	4.03989619	0.00000000	0.00000000
C	3.31682040	1.16390563	0.00000000
C	2.37708633	1.95393431	0.00000000
C	1.18802328	2.53974044	0.00000000
N	-6.78574136	0.00000000	0.00000000
H	-7.29328314	-0.86508701	0.00000000
H	-7.29328314	0.86508701	0.00000000
N	5.48905035	0.00000000	0.00000000
O	6.04274364	-1.07985101	0.00000000
O	6.04274364	1.07985101	0.00000000

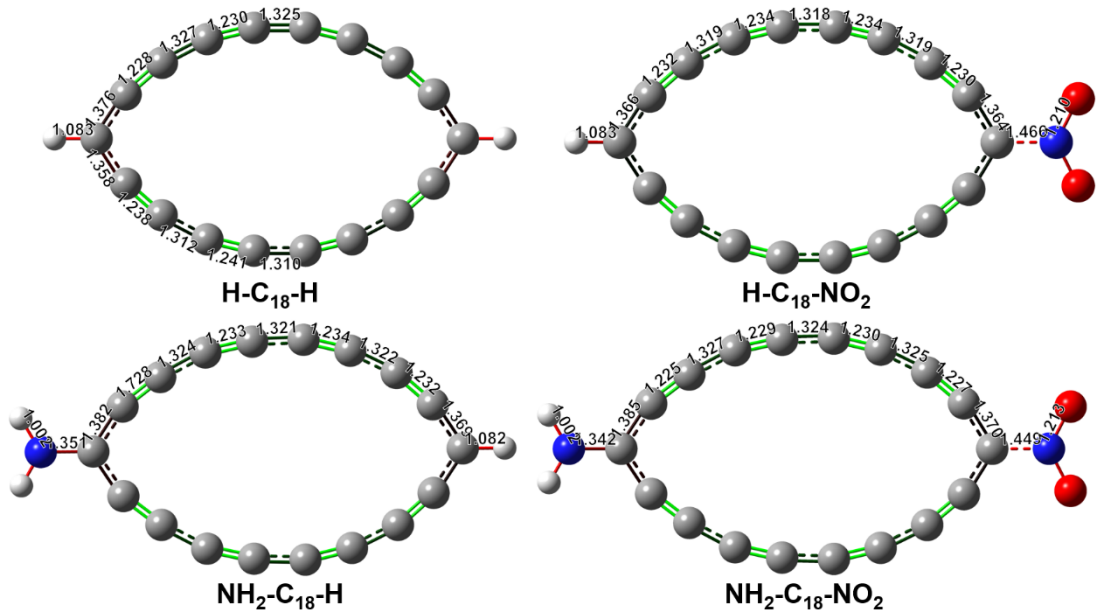


Figure S2. Bond-length colored molecular structure of the studied C₁₈ derivatives. The bond lengths (in Å) are given.

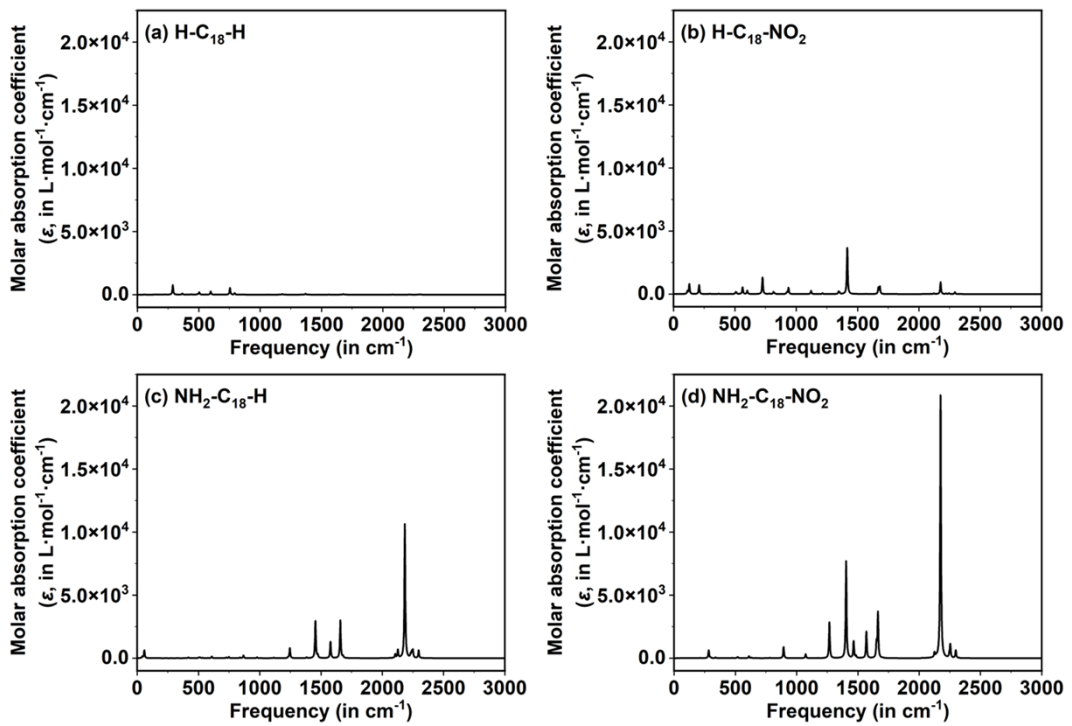


Figure S3. Simulated infrared (IR) spectrum of the studied C₁₈ derivatives. Gaussian function with full width at half-maximum of 8 cm⁻¹ was employed for broadening the theoretical data as spectrum curves.

Table S5. Contributions of the main transition orbitals (MTOs) of crucial excited state involved in maximum wavelength absorption

Molecules	MTOs
H-C ₁₈ -H	HOMO→LUMO (86.1%)
H-C ₁₈ -NO ₂	HOMO→LUMO (89.4%)
NH ₂ -C ₁₈ -H	HOMO→LUMO (88.4%)
NH ₂ -C ₁₈ -NO ₂	HOMO→LUMO (90.3%)

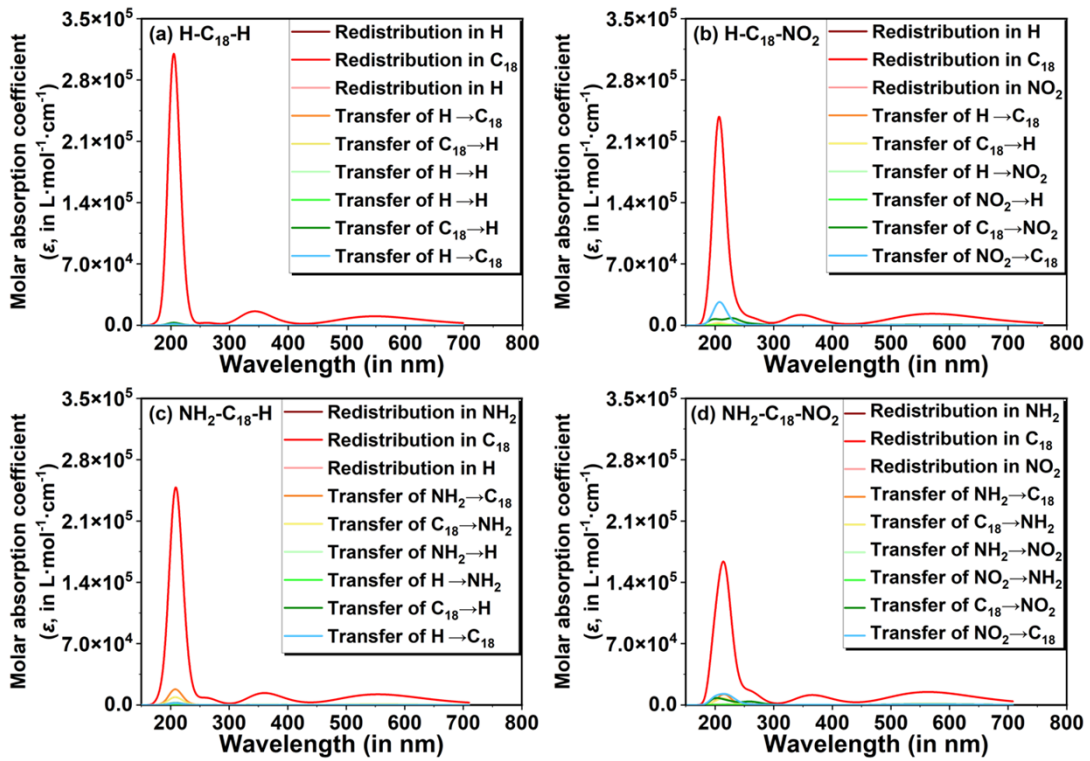


Figure S4. Simulated charge-transfer spectrum (CTS) of the studied C₁₈ derivatives.

The Gaussian function with full width at half-maximum of 0.333 eV was employed for broadening the theoretical data as spectrum curves.

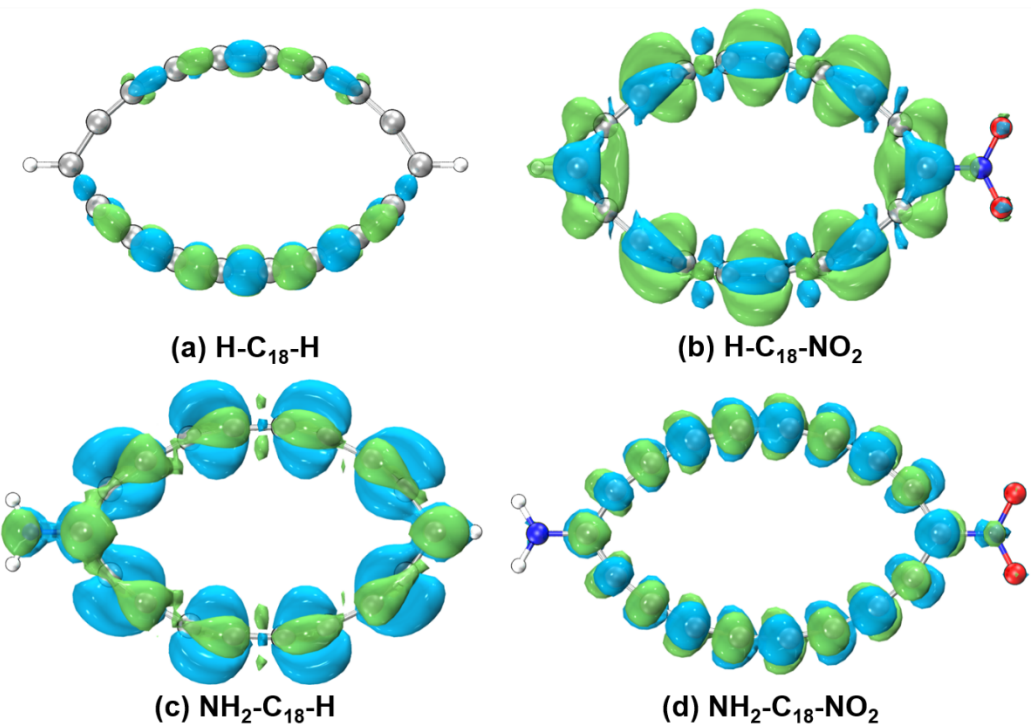


Figure S5. Isosurface maps of electron density difference (EDD) (isovalue = 0.001) of the studied C_{18} derivatives. Green and blue regions denote where electron density is increased and decreased, respectively, after electronic excitation.

Table S6. Transition energy (ΔE , in eV), oscillator strength (f_0), magnitude of the vector difference between the dipole moment of the ground state and those of the excited state ($|\Delta\mu|$, in D), and calculated first hyperpolarizability ($\beta_0^*(-2\omega;\omega,\omega)$, in a.u.) derived from the two-level model for the lowest five excited states of the studied C₁₈ derivatives

	S_n	ΔE	f_0	$ \Delta\mu $	$\beta_0^*(-2\omega;\omega,\omega)$
H-C ₁₈ -H	S ₁	1.88	0.000	2.49	0
	S ₂	2.09	0.026	0.68	16
	S ₃	2.28	0.242	0.20	33
	S ₄	2.43	0.000	1.66	0
	S ₅	2.54	0.001	4.15	1
<hr/>					
NH ₂ -C ₁₈ -H	S ₁	1.85	0.000	0.62	0
	S ₂	2.11	0.001	0.16	0
	S ₃	2.24	0.353	1.24	309
	S ₄	2.2	0.000	0.44	0
	S ₅	2.58	0.000	0.26	0
<hr/>					
H-C ₁₈ -NO ₂	S ₁	1.72	0.000	1.70	0
	S ₂	1.98	0.041	1.78	74
	S ₃	2.19	0.332	4.38	1094
	S ₄	2.39	0.000	2.80	0
	S ₅	2.45	0.000	0.85	0
<hr/>					
NH ₂ -C ₁₈ -NO ₂	S ₁	1.86	0.000	2.93	1
	S ₂	2.10	0.000	3.71	0
	S ₃	2.15	0.002	2.84	4
	S ₄	2.20	0.476	6.37	2252
	S ₅	2.54	0.000	1.26	0

Table S7. Total amounts of the first hyperpolarizability ($\beta_0(-2\omega;\omega,\omega)$, in a.u.), projection of the first hyperpolarizability onto the dipole vector ($\beta_{\text{vec}}(-2\omega;\omega,\omega)$, in a.u.), and Cartesian component of the first hyperpolarizability ($\beta_x(-2\omega;\omega,\omega)$, $\beta_y(-2\omega;\omega,\omega)$, and $\beta_z(-2\omega;\omega,\omega)$, in a.u.) in zero-frequency limit ($\lambda = \infty$ nm) and under frequency-dependent fields ($\lambda = 1907$ and 1460 nm) of the studied C₁₈ derivatives in the gas phase (outside parenthesis) and in cyclohexane solution (inside parenthesis) calculated by analytic derivatives of the system energy (CPKS) method

	λ	$\beta_0(-2\omega;\omega,\omega)$	$\beta_{\text{vec}}(-2\omega;\omega,\omega)$	$\beta_x(-2\omega;\omega,\omega)$	$\beta_y(-2\omega;\omega,\omega)$	$\beta_z(-2\omega;\omega,\omega)$
H-C ₁₈ -H	∞ nm	518 (1019)	-518	0	-518	0
	1907 nm	887 (1841)	-887	0	-887	0
	1460 nm	1622 (3536)	-1622	0	-1622	0
H-C ₁₈ -NO ₂	∞ nm	570 (294)	570	-570	0	0
	1907 nm	773 (124)	773	-773	0	0
	1460 nm	928 (1712)	928	-928	0	0
NH ₂ -C ₁₈ -H	∞ nm	2770 (8234)	-2770	2770	0	0
	1907 nm	4834 (15097)	-4834	4834	0	0
	1460 nm	8487 (28400)	-8487	8487	0	0
NH ₂ -C ₁₈ -NO ₂	∞ nm	4462 (13928)	-4462	4462	0	0
	1907 nm	8107 (26063)	-8107	8107	0	0

-----	1460 nm	15072 (50661)	-15072	15072	0	0
-------	---------	---------------	--------	-------	---	---

Table S8. Tensorial component of the first hyperpolarizability (in a.u.) in the principal axis of the studied C₁₈ derivatives in zero-frequency limit ($\lambda = \infty$ nm) and under frequency-dependent fields ($\lambda = 1907$ and 1460 nm) of the studied C₁₈ derivatives calculated by both analytic derivatives of the system energy (CPKS, outside parenthesis) and finite field (FF, inside parenthesis) methods

	λ	$\beta_{xxy}(-2\omega; \omega, \omega)$	$\beta_{yyy}(-2\omega; \omega, \omega)$	$\beta_{yzz}(-2\omega; \omega, \omega)$
H-C ₁₈ -H	∞ nm	-161	-357 (-352)	-1
	1907 nm	-273	-578	-1
	1460 nm	-461	-1014	-1
	λ	$\beta_{xxx}(-2\omega; \omega, \omega)$	$\beta_{xyy}(-2\omega; \omega, \omega)$	$\beta_{xzz}(-2\omega; \omega, \omega)$
H-C ₁₈ -NO ₂	∞ nm	-937 (-948)	282	85
	1907 nm	-1158	455	101
	1460 nm	-1268	799	126
NH ₂ -C ₁₈ -H	∞ nm	1910 (1910)	881	-21
	1907 nm	3699	1357	-31
	1460 nm	6994	2158	-49
NH ₂ -C ₁₈ -NO ₂	∞ nm	2635 (2612)	1742	84
	1907 nm	5716	2659	98
	1460 nm	11884	4252	116